Disulfide- and Thiol-Incorporating Copper Catenanes: Synthesis, Deposition onto Gold, and Surface Studies

Laurence Raehm,[a] Jean-Marc Kern,*[a] Jean-Pierre Sauvage,*[a] Christine Hamann,[a] Serge Palacin,[b] and Jean-Philippe Bourgoin[b]

Dedicated to Professor Hans J. Schäfer on the occasion of his 65th birthday

Abstract: Two new copper-complexed [2]catenanes have been prepared, both of which consist of two different interlocking rings. In both cases, one of the rings incorporates a disulfide bridge. The other ring contains either a single chelate (phen = 1,10-phenanthroline, a bidentate ligand) or two different chelates (phen and terpy, 2,2′,6′,2″-terpyridine, a tridentate chelate). Deposition of these two complexes on a gold electrode surface was carried out by standard procedures, leading to reductive cleavage of the S–S bridge. The adsorbed species can be viewed as [2]catenanes for which the gold atoms of the electrode surface are an integral fragment of one of the two rings. They yield clear electrochemical responses, but no motion is observed for the catenane incorporating a phen unit and a terpy fragment in one of the two rings, regardless of the metal oxidation state. This is at odds with the behavior of the parent compound in solution, which undergoes ring-gliding motions upon electrochemical reduction or oxidation of the copper center. Near-field microscopy was used to study the deposited layers (STM and AFM). STM images suggest that the molecules do not tend to order at long range on the surface. Polarization modulation–infrared reflection absorption spectroscopy (PM-IRRAS) led to promising results: the two catenanes deposited are likely to be oriented perpendicular to the gold surface.

Keywords: catenanes · molecular devices · monolayers · rotaxanes · self-assembly

Introduction

If bistable molecules, "molecular machines", and switchable systems are to find applications one day, especially in relation to information storage and processing, it is clear that these species will have to be assembled in two- or three-dimensional arrays. A promising possibility is the deposition of the compounds to be used on solid surfaces, allowing subsequent visualization of individual molecules by means of near-field microscopy techniques.

So far, catenanes and rotaxanes represent the best prototypes of molecular machines, that is, multicomponent systems of which certain parts can be set in motion by an external signal, while the other parts can be regarded as motionless.[1, 2] This special feature of interlocked and threaded ring-containing assemblies originates from their special ability to undergo large-amplitude but nondestructive motions in a precisely controlled fashion. Only a few reports have mentioned surface-confined catenanes and rotaxanes so far. The molecules have either been deposited onto an electrode surface by oxidative electropolymerization of pyrrole- or thiophene-substituted precursors (in order to afford a film[3]) or have been adsorbed onto a gold surface by formation of an Au–S bond,[4, 5] following the strategy used very successfully by several groups to make SAMs (self-assembled monolayers).[6] Another promising approach relies on the ability of certain ionic catenanes to form Langmuir films at an air/water interface.[7a] Threading and dethreading of pseudorotaxanes trapped in a rigid matrix or tethered onto a silica film was recently described.[7b]

We would now like to report deposition on a gold surface of two kinds of copper(I)-containing architectures: [2]catenanes incorporating a disulfide bridge in one ring, and pseudorotaxanes whose threaded fragment is end-functionalized by thiol functions. The present paper describes synthesis, adsorption, and electrochemical properties of the compounds in solution as well as when deposited onto the gold surface. In particular we describe a switchable catenane that can easily be

[a] Prof. J.-M. Kern, Dr. J.-P. Sauvage, L. Raehm, C. Hamann
Laboratoire de Chimie Organo-Minérale, UMR 7513 du CNRS
Université Louis Pasteur, Faculté de Chimie
4, rue Blaise Pascal, 67070 Strasbourg Cedex (France)
Fax: (33) 3-90-24-13-68
E-mail: sauvage@chimie.u-strasbg.fr

[b] Dr. S. Palacin, J.-P. Bourgoin
Service de Chimie Moléculaire, CEA Saclay Bât 125
91191 Gif-sur-Yvette Cedex (France)

Supporting information for this article is available on the WWW under http://www.wiley-vch.de/home/chemistry/ or from the author. 1: Infrared spectra of $[Cu\cdot\mathbf{2}]^+$ as a powder (black line, transmission IR spectroscopy) and as a SAM on gold (dotted line, PM-IRRAS). (Spectra offset and scaled for clarity; significant peaks marked with an asterisk.) 2: STM image (819×819 nm^2) of a monolayer of $[Cu\cdot\mathbf{3}]^+$ on Au(111) on mica.

  0947-6539/02/0809-2153 $ 20.00+.50/0

set in motion in solution by the action of an electrochemical signal (Cu^{II}/Cu^{I}). In addition, a set of experiments was carried out to study the behavior of this compound once it was adsorbed onto a gold surface. Surface studies performed on well-characterized surface-immobilized catenanes permitted visualization of the molecules and even the estimation of their relative orientation with respect to the surface.

Results and Discussion

Design, synthesis, and characterization: The three-dimensional template effect of copper(I), introduced almost two decades years ago, made catenanes, rotaxanes, and related systems readily accessible from a preparative point of view.[8] The strategy developed by some of us to prepare catenanes is based on a precursor consisting of two phenanthroline-type ligands entwined around a Cu^{I} center. Indeed, reacting the end functionalities of the acyclic ligands with bifunctionalized molecular links leads to the formation of a catenane. Another strategy, which has been exploited in the present work, consists in using a particular precursor in which one of the ligands is already a macrocycle: the acyclic ligand is threaded through the macrocycle, forming a prerotaxane species before being closed. This alternative strategy is well suited to the synthesis of disymmetrical catenanes or rotaxanes.[9]

These threading steps, involving different coordinating macrocycles and 2,9-diphenyl-1,10-phenanthroline (dpp)-containing acyclic ligands, are represented in Scheme 1 a, b, c. The copper(I) complex $[Cu\cdot\mathbf{1}]^+$ is a pseudorotaxane whose wheel **4** and axle **5** (Scheme 1 a) both incorporate a dpp unit. The axle is end-functionalized by thiol groups at each end, and small alkyl chains have been introduced on the 4- and 7-positions of the phenanthroline unit in order to reduce solubility problems. Pseudorotaxane $[Cu\cdot\mathbf{1}]^+$ was obtained by threading ligand **5**—the axle—through the coordinating macrocycle **4**, using the templating effect of Cu^{I}. Due to the particularly high stability of $[Cu(dpp)_2]$ complexes,[10] the threading step is quantitative. Macrocycle **4**[11] incorporates one bidentate site, a dpp unit. The phenanthroline-attached phenyl groups are joined through a pentaoxoethylene chain,

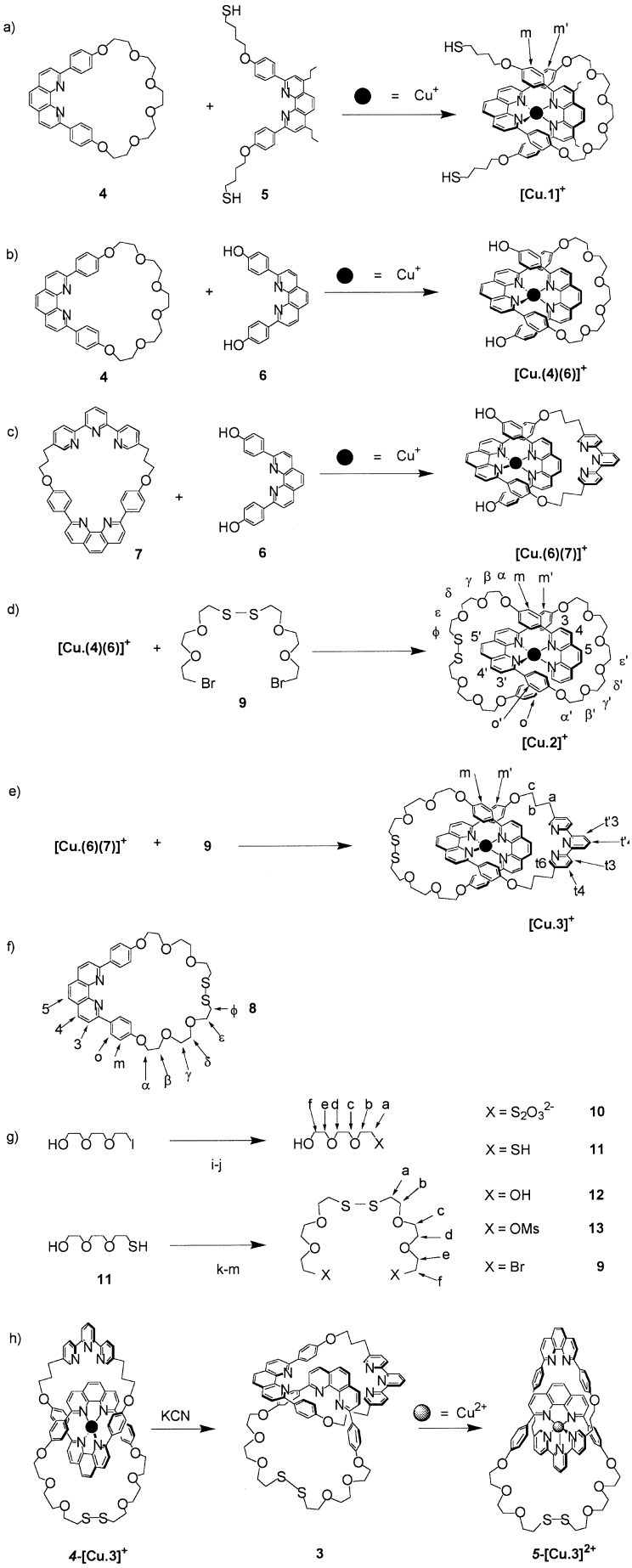

Scheme 1. a) Representation of the threading step leading to prerotaxane $[Cu\cdot\mathbf{1}]^+$. b, c) Threading steps leading to precatenane structures $[Cu(\mathbf{4})(\mathbf{6})]^+$ and $[Cu(\mathbf{6})(\mathbf{7})]^+$. d) Ring-closing reaction leading to the homoleptic catenane $[Cu\cdot\mathbf{2}]^+$. Each macrocycle includes a dpp unit as coordinating site. e) Ring-closing reaction leading to the heteroleptic catenane $[Cu\cdot\mathbf{3}]^+$. One of the rings includes both a bidentate (dpp) and a tridentate (terpy) coordinating site. f) The dpp-based coordinating subunit of $[Cu(\mathbf{4})(\mathbf{6})]^+$ and $[Cu(\mathbf{6})(\mathbf{7})]^+$, which includes a disulfide fragment. Macrocycle **8** is a 34-membered ring. g) Synthetic route leading from 2-[2-(2-iodoethoxy)ethoxy]ethanol to the dielectrophilic reagent **9**: i) sodium thiosulfate, EtOH, reflux, 50%, j) HCl, H_2O, reflux, k) O_2, l) MsCl, NEt_3, $-5\,^{\circ}C$, m) LiBr, acetone, reflux. h) Demetalation of the tetracoordinated Cu(I) catenane and subsequent remetalation with Cu(II) salt leads to the pentacoordinated copper(II) catenane $[Cu\cdot\mathbf{3}]^{2+}$. *The prefixal numbers 4- and 5- (in italics) indicate the coordination numbers.*

0947-6539/02/0809-2154 $ 20.00+.50/0 *Chem. Eur. J.* **2002**, *8*, No. 9

which is linked to the 4,4′-positions through oxygen atoms. Ligand **5** is a bis-*para*-functionalized 4,7-dipropyl-2,9-bis(*p*-hydroxyphenyl)-1,10-phenanthroline. The *para* positions are linked to thiol functionalities by butyl chains.[5a] Owing to its sensitivity towards oxygen, **5** had to be freshly prepared before the threading step leading to $[Cu\cdot\mathbf{1}]^+$ and the adsorption experiments (vide infra). Ligand **5** was prepared by hydrolysis of the stable thioacetate precursor, 4,7-dipropyl-2,9-bis-[*p*-(4-thioacetatobutane-1-oxy)phenyl]-1,10-phenanthroline, the synthesis of which has been previously described.[5a] Compounds $[Cu\cdot(\mathbf{4})(\mathbf{6})]^+$ (Scheme 1b) and $[Cu\cdot(\mathbf{6})(\mathbf{7})]^+$ (Scheme 1c) are the precursors of $[Cu\cdot\mathbf{2}]^+$ (Schemes 2 and 1d) and $[Cu\cdot\mathbf{3}]^+$ (Schemes 2 and 1e). Both $[Cu\cdot\mathbf{2}]^+$ and $[Cu\cdot\mathbf{3}]^+$ are copper [2]catenanes. In $[Cu\cdot\mathbf{2}]^+$, each macrocycle contains the same coordinating fragment, a

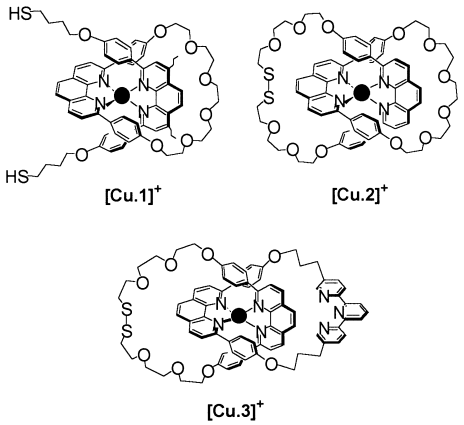

Scheme 2. Pseudorotaxane $[Cu\cdot\mathbf{1}]^+$ and homo- and heteroleptic copper(I) [2]catenanes $[Cu\cdot\mathbf{2}]^+$ and $[Cu\cdot\mathbf{3}]^+$. The axle of the pseudorotaxane is functionalized by thiol groups at each end. Each catenane contains a coordinating ring that includes a disulfide bridge.

dpp unit, but one of the macrocycles, **8** (Scheme 1f), includes a disulfide bridge. This same ring **8** is one of the elements of catenane $[Cu\cdot\mathbf{3}]^+$, in which the second ring **7**[12a] is a heterobischelating macrocycle, including a tridentate site (a terpyridine unit, terpy) and a bidentate site (a phenanthroline unit, dpp). The coordination number of the metal atom, *N*, is clearly defined for $[Cu\cdot\mathbf{2}]^+$ ($N=4$) whatever the oxidation state of the metal is. In contrast, in catenane $[Cu\cdot\mathbf{3}]^+$, the metal can either be tetracoordinated ($N=4$), each macrocycle providing a bidentate unit (dpp), or pentacoordinated ($N=5$), through the dpp core of one ring and the terpy core of the other ring. The first molecular motors developed in our group were based on this ambivalence of the coordination number of the central metal in such systems.[12] Indeed, it was observed that the metal is tetracoordinated in its Cu^I state, each macrocycle providing a dpp unit, but pentacoordinated in the thermodynamically stable situation of the corresponding Cu^{II} catenanes, in which one terpy and one dpp unit surround the metal. The behavior of catenane $[Cu\cdot\mathbf{3}]^{n+}$ after the redox state of the metal has been changed will be described in a later section. Pseudorotaxanes $[Cu(\mathbf{4})(\mathbf{6})]^+$ and $[Cu(\mathbf{6})(\mathbf{7})]^+$ are formed quantitatively by reacting Cu^I ions ($[Cu(CH_3CN)_4]BF_4$ or $[Cu(CH_3CN)_4]PF_6$) with macrocycles **4** and **7**, respectively, in the presence of stoichiometric amounts of 2,9-bis(*p*-hydroxyphenyl)-1,10-phenanthroline (**6**). The ring-closing reactions (Scheme 1d, e) transform these threaded structures into copper [2]catenanes $[Cu\cdot\mathbf{2}]^+$ (15% yield) and $[Cu\cdot\mathbf{3}]^+$ (12% yield), respectively. These reactions lead to the formation of 34-membered macrocycle **8** (Scheme 1f) interlocked with **4** or **7** in $[Cu\cdot\mathbf{2}]^+$ and $[Cu\cdot\mathbf{3}]^+$, respectively. They were achieved by treating the nucleophilic diphenolates corresponding to $[Cu(\mathbf{4})(\mathbf{6})]^+$ and $[Cu(\mathbf{6})(\mathbf{7})]^+$ with the disulfide-bridge-incorporating chain **9** (Scheme 1d, g), which bears an electrophilic carbon at each end. Small amounts of the free macrocycle **8** were isolated in each catenane synthesis. Both sulfur atoms of **9** are linked to a 2-(2-bromoethoxy)ethoxyethyl fragment. The sequential reaction steps leading to **9** from 2-[2-(2-iodoethoxy)ethoxy]-ethanol are represented in Scheme 1g. The free catenane **3** was prepared by demetalation of $[Cu\cdot\mathbf{3}]^+$ with KCN in a ternary acetonitrile/dichloromethane/water solvent[8] (Scheme 1h). Remetalation of the free ligand with $Cu(BF_4)_2$ afforded the copper(II) complex $[Cu\cdot\mathbf{3}]^{2+}$.

Clear evidence of the pseudorotaxane structure of $[Cu\cdot\mathbf{1}]^+$ and of the catenane structures of $[Cu\cdot\mathbf{2}]^+$ and $[Cu\cdot\mathbf{3}]^+$ was obtained by ^1H NMR spectroscopy and FAB-MS. As a consequence of the threading of molecular string **5** through macrocycle **4**, a large upfield shift of the doublets corresponding to the H_m protons (Scheme 1a) of the thread ($\Delta\delta=-1.28$ ppm) and $H_{m'}$ of the macrocycle ($\Delta\delta=-1.09$ ppm) is observed. This shielding effect is characteristic of entwined 2,9-diaryl-1,10-phenanthroline complexes and is due to the spatial proximity of the phenyl group of one coordinating subunit to the phenanthroline core of the other.[13]

Similarly, for $[Cu\cdot\mathbf{2}]^+$ a shielding effect of $\Delta\delta=-1.21$ ppm is observed for the *meta* protons $H_{m'}$ compared to the corresponding protons in free ring **4** (Figure 1). A similar shift is observed after the threading process for protons H_m of the disulfide bridge containing macrocycle **8**. For $[Cu\cdot\mathbf{3}]^+$, in which one ring, **7**, incorporates two different coordinating sites, ^1H NMR confirms at once the catenane structure and the entwining of two dpp subunits (one from each macrocycle) around the metal. Indeed, the upfield shifts of protons H_m and $H_{m'}$ ($\Delta\delta=-1.10$ ppm for H_m and -1.17 ppm for $H_{m'}$) are close to those observed for the analogous protons in $[Cu\cdot\mathbf{2}]^+$, whereas protons of the terpyridine subunit in $[Cu\cdot\mathbf{3}]^+$ resonate at a similar field to those in free macrocycle **7**. FAB-MS of pseudorotaxane $[Cu\cdot\mathbf{1}]^+$ reveals the threaded structure of this molecular assembly: intense peaks are observed which correspond to the loss of the counterion ($m/z=1253.0$ for $[Cu\cdot\mathbf{1}^+]$), to the loss of both counterion and thread ($m/z=629.4$ for $[Cu\cdot\mathbf{1}^+-\mathbf{5}]$) and to the loss of counterion, thread, and metal to leave the macrocycle **4** ($m/z=567.6$ for $[\mathbf{4}^+{+}H]$).

The positive FAB mass spectra of $[Cu\cdot\mathbf{2}]^+$ and $[Cu\cdot\mathbf{3}]^+$ show a pattern that has already been observed for other metallocatenanes. A characteristic feature of the mass spectra of catenanes is the almost total absence of ions between the molecular peak and the peak corresponding to one individual macrocycle.[14] Thus for $[Cu\cdot\mathbf{2}]^+$ the spectrum shows the molecular peak ($[Cu\cdot\mathbf{2}^+]$ $m/z=1287.3$), and the next highest peaks are those of each of the constituent macrocycles complexed by a copper(I) ion, namely $[Cu{+}\mathbf{4}^+]$ ($m/z=629.2$) and $[Cu{+}\mathbf{8}^+]$ ($m/z=721.2$), respectively. Figure 2 displays the

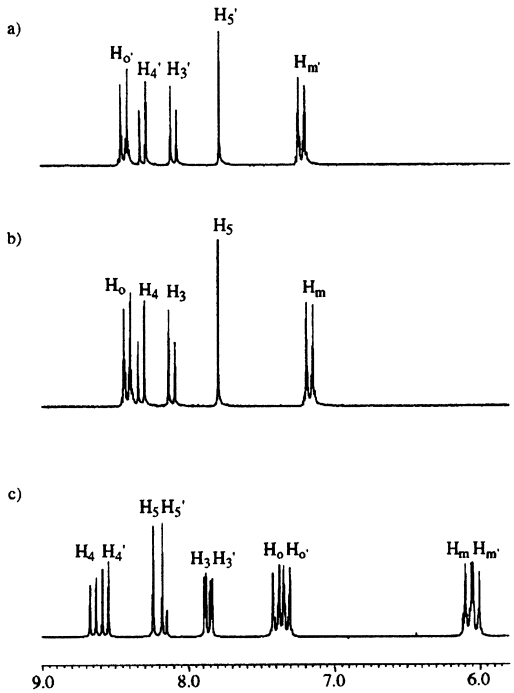

Figure 1. The upfield shielding of protons H_o and H_m in the copper catenanes: representation of the aromatic region of the ^1H NMR spectra of catenane $[Cu\cdot\mathbf{2}]^+$ (spectrum c) and of its metal-free constituent rings **4** (spectrum b) and **8** (spectrum a).

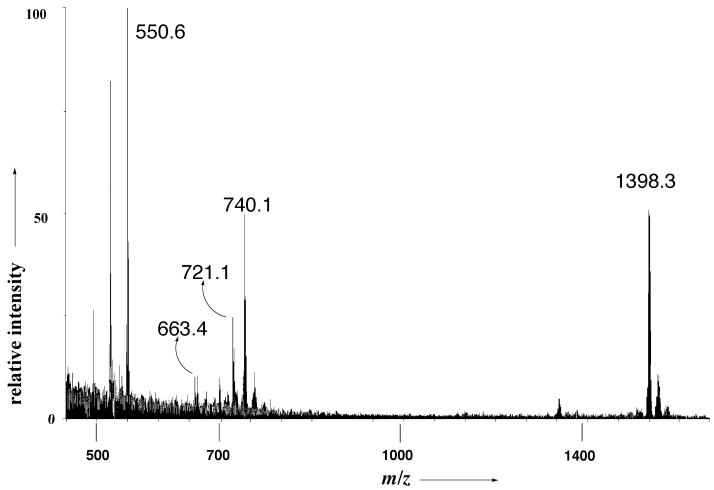

Figure 2. FAB-MS spectrum of the heteroleptic catenane $[Cu\cdot\mathbf{3}]^+$. Fragmentation of the copper(I) catenane $[Cu\cdot\mathbf{3}]^+$ ($m/z = 1398.3$) leads to the formation of $[Cu{+}\mathbf{7}^+]$ ($m/z = 740.1$) and $[Cu{+}\mathbf{8}^+]$ ($m/z = 721.1$).

FAB mass spectrum of catenane $[Cu\cdot\mathbf{3}]^+$. The main peaks correspond to $[Cu\cdot\mathbf{3}^+]$ ($m/z = 1398.3$), $[Cu{+}\mathbf{7}^+]$ ($m/z = 740.1$), and $[Cu{+}\mathbf{8}^+]$ ($m/z = 721.1$).

Deposition on a gold surface and electrochemical studies: In the field of self-assembled monolayers, numerous authors have taken advantage of the strong interaction between sulfur atoms and gold.[6] The presence of thiol or disulfide functionalities in the compounds studied here permitted their attachment to a gold surface.

The electrochemical properties of both the free and the adsorbed species are due to the copper center. The reversible Cu^{II}/Cu^{I} transition occurs in two different potential ranges, depending on the coordination sphere of the metal. Thus, for complexes in which copper(I) is coordinated to two dpp units, that is, $[Cu(dpp)_2]^+$, where the metal is tetracoordinated and the monovalent state is strongly stabilized, oxidation of the metal occurs between 0.55 and 0.70 V versus SCE.[15] In contrast, in complexes where Cu^{II} is stabilized by five nitrogen atoms (one bidentate and one tridentate ligand), a dramatic cathodic shift ($\Delta E \sim -0.7$ V) is observed for the oxidation potential of the monovalent state.[8] Fortunately, this potential window is compatible with the SAM and no damage to the self-assembled monolayers was observed (vide infra) when the applied potential was in this range. Thus, the electroactivity of the complexes allowed us to monitor the adsorption process by cyclic voltammetry (CV). Adsorption was achieved by immersing gold bead electrodes in dichloromethane solutions of $[Cu\cdot\mathbf{1}]^+$, $[Cu\cdot\mathbf{2}]^+$, or $[Cu\cdot\mathbf{3}]^+$. After the adsorption time, the gold beads were thoroughly rinsed with CH_2Cl_2, dipped into dichloromethane containing only Bu_4NBF_4 as supporting electrolyte, and used as working electrodes. Figure 3a depicts the characteristic CV curves obtained after dipping a gold bead into a solution of $[Cu\cdot\mathbf{1}]^+$. Figure 3b illustrates, for comparison, the electrochemical response of the threaded complex $[Cu\cdot\mathbf{1}]^+$ in solution.

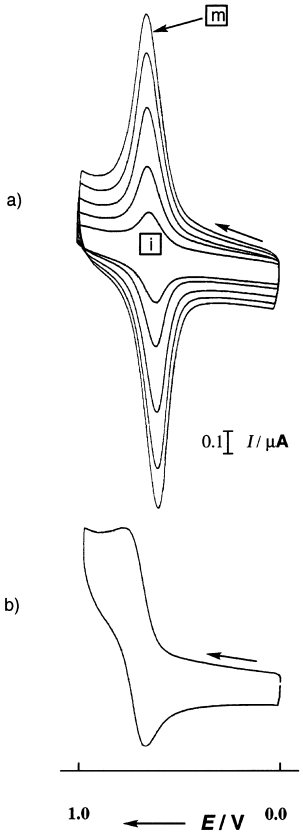

Figure 3. a) Cyclic voltammetric response of a gold bead electrode (CH_2Cl_2, 10^{-1} mol L^{-1} Bu_4NBF_4) after being dipped (20 min) in a solution of prerotaxane $[Cu\cdot\mathbf{1}]^+$ (10^{-3} mol L^{-1}) in CH_2Cl_2 and rinsed. The potential scan rate was successively increased from 50 mV s^{-1} (curve i) to 400 mV s^{-1} (curve m). b) Cyclic voltammetric response of the same complex $[Cu\cdot\mathbf{1}]^+$ in solution (CH_2Cl_2, 10^{-1} mol L^{-1} $n$$Bu_4NBF_4$, Pt electrode, 0.5 mmol L^{-1}, potential sweep rate: 100 mV s^{-1}).

  0947-6539/02/0809-2156 $ 20.00+.50/0 *Chem. Eur. J.* **2002**, *8*, No. 9

In Figure 3a, the presence of a reversible electron transfer at 0.61 V versus silver quasireference is evident. This potential corresponds to the oxidation/reduction process of the bisdiarylphenanthroline Cu^{I} moiety. The difference in potential (ΔEp) between oxidation and reduction peaks is less than 60 mV (30 mV at a sweep rate of 100 mV s^{-1}) and no broadening of ΔEp was observed when the potential sweep rate v was increased (v was varied from 50 to 400 mV s^{-1}; curves i–m in Figure 3a). This is characteristic of surface-confined species. The intensity of the anodic and cathodic peak current increases linearly with the sweep rate v, as expected too for a reversible anchored redox species. The stability of the adsorbed complex is remarkable; less than 15% decrease in electroactivity was observed after 60 cycles. The adsorption process itself is fast, and the coverage of the gold surface can reach its maximum value as soon as after 15 minutes dipping.

The electrochemical response of a gold bead electrode after it had been dipped in a solution containing a copper(I) threaded complex evidences the adsorption of a bis-dpp structure onto the surface. Undoubtedly, this strong adsorption, as shown by the stability of the electrochemical response, is a consequence of Au–S bond formation. Indeed, adsorption experiments using similar structures but free of thiol functions led only to weak and unstable electrode coverages.

As a consequence of the adsorption of the thiol functions of the thread of the Cu^{I} prerotaxane $[Cu\cdot\mathbf{1}]^{+}$, the gold-adsorbed species can be viewed as a [2]catenane in which the gold atoms of the surface are an integral part of one of the rings (Scheme 3a). In this particular catenane, the gold atoms are part of the assembly. They act as a link between the two ends of the thread, converting a rotaxane-like assembly to a catenane one. However, due to the pronounced reducing character of the thiol functionality, only the copper(I) prerotaxane can be prepared and consequently adsorbed. The corresponding copper(II) rotaxane is too strong an oxidant to be compatible with the presence of thiol functionalities in the molecular structure. The reducing power of the thiol functionalities also explains the low stability of $[Cu\cdot\mathbf{1}]^{+}$ and of the free molecular thread **5** in the presence of air, which leads progressively to the formation of insoluble polydisulfide material. Going from the threaded structure $[Cu\cdot\mathbf{1}]^{+}$ to the catenane structure $[Cu\cdot\mathbf{2}]^{+}$ or $[Cu\cdot\mathbf{3}]^{+}$ allowed us to overcome these difficulties. Indeed, the disulfide bridge present in **8**, which is one of the constituent rings of both catenanes $[Cu\cdot\mathbf{2}]^{+}$ and $[Cu\cdot\mathbf{3}]^{+}$, is chemically inert towards oxidation and will act as an alternative to the thiol functionality in the adsorption process. Moreover, mechanical linkage of the rings in the catenanes excludes the possibility of ligand exchange around the metal in the course of the adsorption process. The electrochemical behavior of the molecular catenane $[Cu\cdot\mathbf{2}]^{+}$ is as expected for a dpp-based copper catenane.[15] The reversible redox process occurs at 0.69 V versus a silver quasireference electrode. An adsorption phenomenon was observed when a gold bead electrode was dipped into a solution of $[Cu\cdot\mathbf{2}]^{+}$. This was evidenced by the persistence of the redox signal centered at 0.58 V after the electrode had been treated as described above. Here again, the redox signal is attributed to the $[Cu^{II}(dpp)_2]/[Cu^{I}(dpp)_2]$ transition, and the

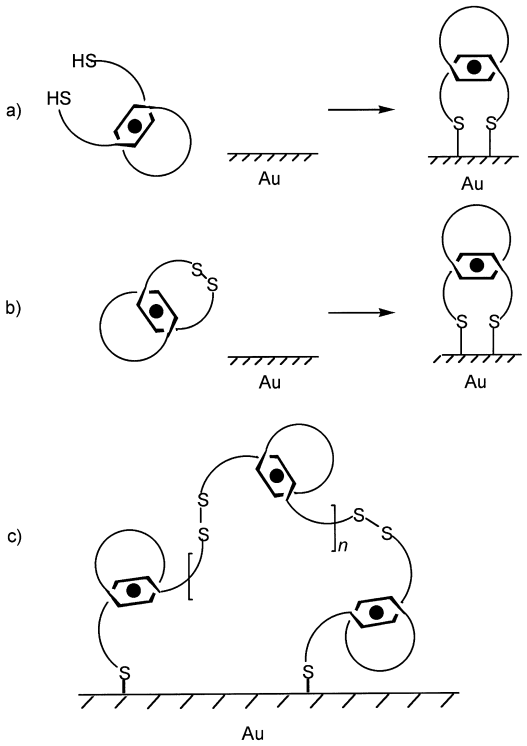

Scheme 3. Schematic representation of the adsorption processes leading: a) from a pseudorotaxane structure to a catenane state; b) from a molecular catenane to a surface-confined catenane in which gold atoms are constituent elements of one ring; c) from polydisulfide material formed in solution by oxidation of the thiol functions of the pseudorotaxane $[Cu\cdot\mathbf{1}]^{+}$ to immobilized polyrotaxanes.

electrochemical response of the modified electrode is very similar to that observed after adsorption of $[Cu\cdot\mathbf{1}]^{+}$: a potential difference between oxidation and reduction peaks inferior to 60 mV ($\Delta Ep = 20$ mV), linear increase of the intensity of the redox signals with the potential sweep (50 to 400 mV s^{-1}) but no modification of the potential of the oxidation and reduction peaks. But in that case the adsorption process represented schematically in Scheme 3b leads from a molecular catenane in solution to a surface-anchored one. During this transformation, the disulfide bridge of ring **8** is likely to be cleaved,[16], leading to two Au–S bonds. Consequently, ring **8** is converted into a new species, which can again be considered as a well-defined macrocycle, but in which gold atoms are constituent elements of the ring.

In solution, the electrochemical behavior of $[Cu\cdot\mathbf{3}]^{+}$ is markedly different from those of $[Cu\cdot\mathbf{1}]^{+}$ and $[Cu\cdot\mathbf{2}]^{+}$. Indeed, one of the rings, ring **7**, of this catenane includes two different coordinating sites, a dpp and a terpy unit. Owing to the pronounced difference of the stereoelectronic requirements of copper(I) and copper(II), a reorganization of the coordination sphere of the metal, and subsequently of the rings around the metal, could be expected after the change in its redox state.[17]

Figure 4a illustrates the electrochemical behavior of $[Cu\cdot\mathbf{3}]^{+}$ in a Et_4NBF_4 acetonitrile solution. The signal occurring at 0.71 V corresponds to the tetracoordinate $Cu^{II/I}$ couple and is in accordance with the ^1H NMR observations, which indicate that two dpp units (each macrocycle included

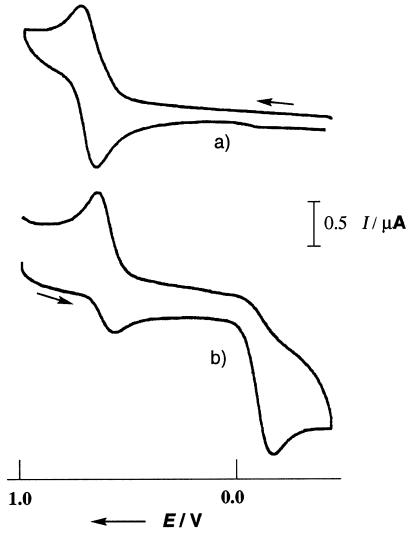

Figure 4. Cyclic voltammetry curves recorded with a Pt working electrode at sweep rate 50 mV s^{-1} (CH_3CN, 10^{-1} mol L^{-1} Bu_4NBF_4, Ag wire pseudoreference): a) tetracoordinated copper(I) catenane *4*-$[Cu\cdot\mathbf{3}]^+$; b) chemically prepared pentacoordinated copper(II) catenane *5*-$[Cu\cdot\mathbf{3}]^{2+}$.

in $[Cu\cdot\mathbf{3}]^+$ providing one unit) are entwined around the metal (vide supra). In addition, it can be observed that the intensities of the cathodic and anodic peaks are equal, showing that no transformation or reorganization of the tetracoordinated Cu^{II} complex (formed in the diffusion layer during the oxidation process) occurs on the time scale of the measurement (potential sweep rate: 100 mV s^{-1}).

In contrast, the corresponding Cu^{II} catenane $[Cu\cdot\mathbf{3}]^{2+}$ prepared by metalation of the free ligand **3** behaves very differently in solution (Figure 4b). In the experiment represented in Figure 4b, the potential sweep was started at +1.0 V, a potential at which no electron transfer should occur, whatever the surroundings of the central Cu^{II} are (penta- or tetracoordination). The curve, recorded at 100 mV s^{-1}, has two cathodic peaks: a small one located at +0.60 V followed by an intense one at −0.13 V. Only one anodic peak, at 0.67 V, appears during the reverse sweep. The weak peak at 0.60 V is due to the presence of small quantities of tetrahedral $[Cu\cdot\mathbf{3}]^+$. Indeed, in the preparation of $[Cu\cdot\mathbf{3}]^{2+}$, we always observed the formation of a small proportion of the Cu^I catenane. This phenomenon is probably due to the presence of trace amounts of organic electron donors or to a small proportion of ligand acting as an irreversible reducing agent. The main cathodic peak at −0.13 V is characteristic of pentacoordinated Cu^{II}. These observations confirm that in $[Cu\cdot\mathbf{3}]^{2+}$ prepared by metalation of the free catenane with Cu^{II} ions the central metal is coordinated to the tridentate terpy site of ring **7** and to the bidentate dpp site of ring **8**. The irreversibility of this peak means that the pentacoordinated Cu^I species formed in the diffusion layer when the potential is swept cathodically is transformed very rapidly and in any case before the electrode potential becomes more anodic than the potential of the pentacoordinated Cu^{II}/Cu^I redox system. The irreversible character of the wave at −0.13 V and the appearance of an anodic peak at the value of +0.60 V indicates that the transient species formed by reduction of pentahedral *5*-$[Cu\cdot\mathbf{3}]^{2+}$ (*5* indicating the coordination number of the metal) has undergone a complete rearrangement that leads to a tetracoordinated Cu^I catenane. These two complementary cyclic voltammetry experiments confirm that in this catenane, as in previously studied related systems,[12] the tetracoordinated Cu^I state is more stable than the pentacoordinated one, and the pentacoordinated Cu^{II} state is more stable than the tetracoordinated one. Moreover, it was observed that the rearrangement rates from the less to the more stable geometries are dramatically different for the two oxidation states of the metal: although the isomerization of *5*-$[Cu\cdot\mathbf{3}]^+$ into *4*-$[Cu\cdot\mathbf{3}]^+$ occurs on the same time scale as the cyclic voltammetry, the rearrangement of *4*-$[Cu\cdot\mathbf{3}]^{2+}$ into the thermodynamically more stable species, *5*-$[Cu\cdot\mathbf{3}]^{2+}$, is too slow to be monitored by this electrochemical technique.

Triggering intramolecular motions in immobilized species at will is a challenging target. From a structural point of view, this should be possible with the gold-adsorbed $[Cu\cdot\mathbf{3}]^{n+}$ species. Two sets of experiments were performed in order to check whether catenane-containing SAMs are suitable candidates for the elaboration of surface-attached molecular devices. In a first series, $[Cu\cdot\mathbf{3}]^+$ was adsorbed onto a gold bead. The adsorption process took place as for $[Cu\cdot\mathbf{1}]^+$ or $[Cu\cdot\mathbf{2}]^+$, as illustrated in Figure 5a. This modified electrode was polarized at 1.0 V, and CV curves were recorded at

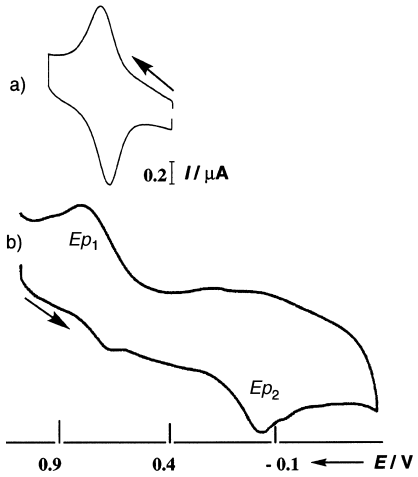

Figure 5. a) Cyclic voltammetric response of a gold bead electrode: a) after dipping (15 min) in a solution of $[Cu\cdot\mathbf{3}]^+$ and rinsing; b) after dipping (18 h) in a solution of $[Cu\cdot\mathbf{3}]^{2+}$ and rinsing. Medium: CH_2Cl_2, 10^{-1} mol L^{-1} Bu_4NBF_4. Potential sweep rate: 50 mV s^{-1}.

regular intervals. These curves remained unchanged from that represented in Figure 5a, which was recorded immediately after the adsorption step. Observations made with the surface-confined species underline the kinetic inertness of tetracoordinated *4*-$[Cu\cdot\mathbf{3}]^{2+}$ and are similar to those made with $[Cu\cdot\mathbf{3}]^+$ in solution. In a second run, chemically prepared *5*-$[Cu\cdot\mathbf{3}]^{2+}$, in which the metal has a pentacoordinated environment, was adsorbed on gold by means of the same procedure as for $[Cu\cdot\mathbf{1}]^+$ and $[Cu\cdot\mathbf{2}]^+$. In order to observe movements inside the SAM, the potential sweep was started at +0.9 V, a potential at which no electron transfer should occur, regardless of the surroundings of the copper center, in other words, whether there are four or five coordinated atoms.

  0947-6539/02/0809-2158 $ 20.00+.50/0 *Chem. Eur. J.* **2002**, *8*, No. 9

CV measurements evidenced the formation of an electroactive layer on the gold surface. Despite the fact that the waves are less well defined, it is clear from Figure 5b that two redox systems, called Ep_1 and Ep_2, are present. The potential difference between these two systems is nearly the same as that observed for the $[Cu(dpp)_2]^{2+/+}$ and $[Cu(dpp, terpy)]^{2+/+}$ moieties in solution. In the previous section it was emphasized that the preparation of *5*-$[Cu\cdot\mathbf{3}]^{2+}$ is accompanied by the formation of *4*-$[Cu\cdot\mathbf{3}]^{+}$, a fact that may explain the presence of wave Ep_1 in Figure 5b. Assuming that the more cathodically located wave Ep_2 corresponds to the reduction of adsorbed *5*-$[Cu\cdot\mathbf{3}]^{2+}$, polarization of the modified electrode at a potential more negative than Ep_2 should lead to the reduction of the whole SAM including the pentacoordinated Cu^{II} catenane. The electrochemical study of *5*-$[Cu\cdot\mathbf{3}]^{2+}$ in solution showed that *5*-$[Cu\cdot\mathbf{3}]^{+}$ is less stable than *4*-$[Cu\cdot\mathbf{3}]^{+}$, and that electrogeneration of *5*-$[Cu\cdot\mathbf{3}]^{+}$ is rapidly followed by its transformation to the thermodynamically more stable linkage isomer *4*-$[Cu\cdot\mathbf{3}]^{+}$. If the same process occurred for anchored *5*-$[Cu\cdot\mathbf{3}]^{+}$, an increase in the intensity of Ep_1 and a decrease in that of Ep_2 would be expected when successive cyclic potential scans from positive to negative values were carried out with the Au–*5*-$[Cu\cdot\mathbf{3}]^{2+}$ entity. However, even when the potential was scanned slowly ($50\,mV\,s^{-1}$) and continuously from 1.0 to -0.3 V and vice versa, or even when the electrode potential was polarized at -0.3 V for 120 s, no modification of the shape of the CV curves was observed. In particular, no peak increase of the Ep_1 intensity was observed when scanning cathodically from 0.9 V at the second scan. These experiments seem to indicate that intramolecular motions in this surface-confined pentacoordinated Cu^{I} catenane are markedly slowed down in comparison with the molecular species in solution, if not totally frozen.

Surface studies: Electrochemical studies evidenced the adsorption on gold of threaded and interlocked copper complexes. Knowledge of the coverage ratio of the host metal gives useful information on the formation of mono- or multilayers. The organization of the layer(s) was investigated by AFM (atomic force microscopy) and STM (scanning tunneling microscopy) techniques. PM-IRRAS (polarization modulation–infrared reflection absorption spectroscopy) was used to collect information about the orientation of the adsorbed species on the surface.

The roughness factor of the gold surface was determined by iodine chemisorption[18] to give the developed area of the electrode. The amount of electroactive species deposited onto the metal was simply deduced from the CV curves by determination of the quantity of current needed for oxidation and/or reduction of the SAM. The area occupied by adsorbates on the surface was determined by projection of their CPK models onto a plane and was estimated to be roughly 280 $Å^2$. The corresponding diameter of the adsorbates ($\sim$19 Å) is in accordance with the size of the dots observed by STM (vide infra). The coverage ratio τ was then obtained by division of the surface area of the SAM by the developed surface area of the electrode. For threaded complex $[Cu\cdot\mathbf{1}]^{+}$, in which a thiol group is attached at each end of the axle, evaluation of the coverage ratio τ led to values superior to 100%. On the other hand, the relatively low τ value (43%) obtained in the case of $[Cu\cdot\mathbf{2}]^{+}$ is an indication that the adsorption process of this complex does not lead to a compact layer on the gold surface. For $[Cu\cdot\mathbf{1}]^{+}$, the τ value is abnormally high, suggesting that more than one monolayer of adsorbed $[Cu\cdot\mathbf{1}]^{+}$ is anchored to the gold surface. This observation could be related to the chemical instability of $[Cu\cdot\mathbf{1}]^{+}$ mentioned in the previous section. Indeed, the polydisulfide material obtained by oxidation of the thiol end groups can adsorb onto gold, either through some disulfide bridges present in the structure or through the thiol functionalities. The coverage ratio being based on the intensity of the electrochemical response of the copper centers present on the electrode surface, the adsorption of oligomers of $[Cu\cdot\mathbf{1}]^{+}$ can actually yield τ values larger than 1 (Scheme 3c).

Infrared analysis of $[Cu\cdot\mathbf{3}]^{+}$ SAM on gold: Figure 6 shows the PM-IRRAS spectrum of a monolayer of $[Cu\cdot\mathbf{3}]^{+}$ on gold, together with the transmission IR spectrum of the same compound as a powder (KBr pellet). Several peaks (at 1538, 1458, 1360, and 1330 cm^{-1}, for example) appear significantly more intense with respect to the other peaks in the PM-IRRAS spectrum than in the transmission IR spectrum. These peaks are likely to arise from in-plane transition moments coming from the aromatic groups of the molecule: phenanthroline, pyridine, or phenyl groups.[19, 20] As PM-IRRAS is only sensitive to transition dipolar moments perpendicular to the metal surface, these aromatic groups are likely to be oriented perpendicular to the plane of the substrate. Thus, the $[Cu\cdot\mathbf{3}]^{+}$ molecule is likely to adsorb on gold with its two rings roughly perpendicular to the gold surface.

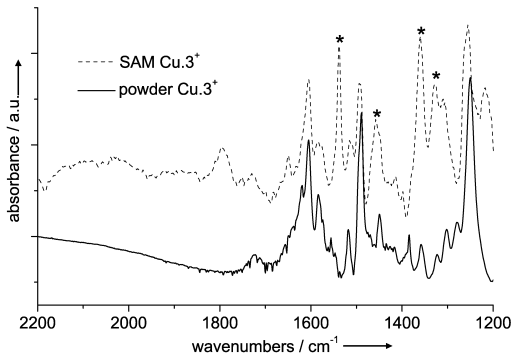

Figure 6. Infrared spectra of $[Cu\cdot\mathbf{3}]^{+}$ as a powder (unbroken line, transmission IR spectroscopy) and as a SAM on gold (dotted line, PM-IRRAS). The spectra are offset and scaled for clarity. Significant peaks are marked with an asterisk.

Similar conclusions can be obtained from the IR and PM-IRRAS spectra of catenane $[Cu\cdot\mathbf{2}]^{+}$ in the powder state and as a SAM on a gold surface. This molecule is likely to be oriented perpendicularly to the gold surface as $[Cu\cdot\mathbf{3}]^{+}$. These observations are important since they demonstrate that a certain level of geometrical control can be reached at the electrode surface.

AFM and STM investigation of $[Cu\cdot\mathbf{3}]^{+}$ SAM on gold: STM and AFM were used to characterize the texture of the film

formed by adsorption of catenane molecules $[Cu\cdot\mathbf{3}]^+$ onto gold surfaces (adsorption time 15 min). As shown in Figure 7, the adsorbed molecules form a homogeneous layer with a slightly grainy texture.

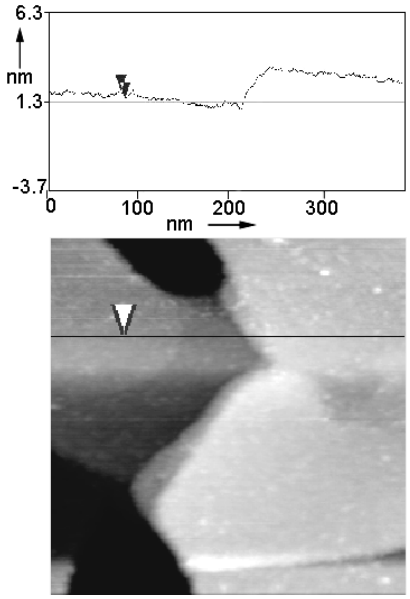

Figure 7. Tapping-mode image ($387\times387\,nm^2$) of a layer of $[Cu\cdot\mathbf{3}]^+$ molecules on a gold substrate. The vertical distance between the markers is 0.36 nm.

Large-scale STM images (available as Supporting Information) confirm that the layer is homogeneous in terms of electron transmission properties too. At some places some holes were observed in the layer, as shown in Figure 8a. The figure also corroborates the AFM data concerning the grainy texture. The absence of grainy texture in the black areas, together with the homogeneity of the layer over a large area, seems to indicate that a monolayer is formed. At lower imaging current, it was possible to resolve the grainy structure by STM. This is shown in Figure 8b. Though the image is noisy, a fine texture consisting of dots of the same gross size is visible. These dots are 2–3 nm in diameter, which is comparable to the expected size of a $[Cu\cdot\mathbf{3}]^+$ molecule. Taking this into account along with the fact that the images were stable with time, we believe that these dots may correspond to individual $[Cu\cdot\mathbf{3}]^+$ molecules. No long-range ordering of these molecules was found. At some places, however, a compact or a square arrangement was observed, but never involving more than 8–10 molecules.

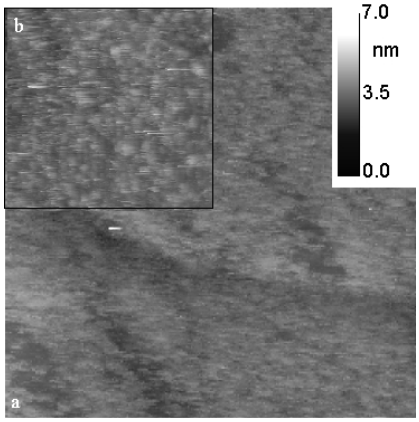

Figure 8. a) STM image ($203\times203\,nm^2$) of a layer of $[Cu\cdot\mathbf{3}]^+$ molecules on a gold substrate. $V_t=916$ mV, $I_t=57$ pA. The black area corresponds to holes in the layer of molecules. b) The inset shows a different place (100×100 nm) on the same layer with different imaging conditions : $V_t=550$ mV, $I_t=2.5$ pA.

Conclusion

In this work a strategy to form surface-bound dynamic systems was explored. The synthesis of a diphenyl-based copper(I) prerotaxane and two copper catenanes has been described. Grafting of thiol functionalities onto both ends of the axle of the prerotaxane allowed its adsorption onto a gold surface and the formation of a hybrid architecture in which atoms of the metal electrode belong to one of the rings of the catenane. Similarly, adsorption of molecular copper catenanes in which one ring includes a disulfide bridge leads to SAMs. In the particular case of the heteroleptic copper catenane $[Cu\cdot\mathbf{3}]^+$, in which one ring includes a bidentate site and a tridentate site, the bistability was investigated by cyclic voltammetry. As for previously described analogous systems, a great difference was observed between the kinetic stability of pentacoordinated Cu(I) catenanes and that of tetracoordinated Cu(II) catenanes. In the case of the adsorbed species, the bistable phenomenon could not be demonstrated, whereas it could for the molecular catenanes in solution. Near-field microscopy techniques, AFM and STM, allowed observation of the monolayers formed by the adsorbed molecules, in which nevertheless there was no long-range order visible. PM-IRRAS studies of the surface-confined catenanes provided interesting information about the relative orientations of the interlocked rings, which are both roughly perpendicular to the surface.

Experimental Section

General methods: Oxygen or water-sensitive reactions were conducted under a positive pressure of argon in oven-dried glassware, by Schlenk techniques. Common reagents and materials were purchased from commercial sources. The following materials were prepared according to literature procedures: $[Cu\cdot\mathbf{1}]^+$,[5a] **4**,[11] **5**,[5a] **6**,[11] **7**,[12a] $[Cu(CH_3CN)_4BF_4]$,[21] $[Cu(CH_3CN)_4PF_6]$,[22] and 2-[2-(2-iodoethoxy)ethoxy]ethanol.[23] Column chromatography was carried out on silica gel 60 (E. Merck, 70–230 mesh). ^{1}H NMR spectra were obtained on either a Bruker WP200SY (200 MHz) or an AM400 (400 MHz) spectrometer. NMR chemical shifts δ are expressed relative to internal solvent peaks. The coupling constants J are measured in Hz. Labels for the protons of the prerotaxane $[Cu\cdot\mathbf{1}]^+$, the [2]catenanes $[Cu\cdot\mathbf{2}]^+$ and $[Cu\cdot\mathbf{3}]^+$, and their precursors are provided in Scheme 1. Fast-atom bombardment mass spectrometry (FAB MS) data were recorded in the positive ion mode with a xenon primary atom beam in conjunction with a 3-nitrobenzyl alcohol matrix and a ZAB-HF mass spectrometer. A VG BIOQ triple quadrupole spectrometer was used for the electrospray mass spectrometry measurements (ES-MS), also in the positive ion mode.

2-[2-(2-Sodiothiosulfatoethoxy)ethoxy]ethanol (10, Bunte salt): A solution of pentahydrated sodium thiosulfate (7.13 g, 28.3 mmol) in water (20 mL) was added to a refluxing solution of 2-[2-(2-iodoethoxy)ethoxy]ethanol

  0947-6539/02/0809-2160 $ 20.00+.50/0 *Chem. Eur. J.* **2002**, *8*, No. 9

(5.72 g, 21.9 mmol) in ethanol (30 mL). After the solvents had been removed, the residue was taken up in ethanol and filtered to eliminate the remaining sodium thiosulfate. The solvent was then removed and cold acetone was added to dissolve the sodium iodide produced by the reaction. The product was filtered and dried. The isolated white crystals (5.11 g) contained approximately 40% sodium iodine (estimated by ES-MS), which gives a rough 50% yield for the reaction. White solid; ^{1}H NMR (200 MHz, $CDCl_3$): $\delta = 3.82$ (t, $^3J(H,H) = 6.7$ Hz, 2H; H_f), 3.6–3.4 (m, 8H; $H_{b,c,d,e}$), 3.17 (t, $^3J = 6.6$ Hz, 2H; H_a).

2-[2-(2-Mercaptoethoxy)ethoxy]-ethanol (11) and 2-{2-[2-{2-[2-(2-hydroxyethoxy)ethoxy]ethyldisulfanyl}ethoxy}ethoxy]ethanol (12): A solution of molar hydrochloric acid (40 mL, 0.04 mol) was added to a solution of **10** (3.208 g, 11.9 mmol) in 10 mL ethanol and left for 15 hours. The solvents were then removed and the residue was taken up in CH_2Cl_2/H_2O. The thiol **11** was extracted with CH_2Cl_2 and the organic layer stirred in the presence of air over one night without further purification of **11**. After removing the solvent, the resulting dark orange oil was purified by flash column chromatography (SiO_2, eluent CH_2Cl_2/MeOH 2%). The product was isolated (1.11 g) in quantitative yield.

Compound 12: Yellow oil; ^{1}H NMR (200 MHz, $CDCl_3$): $\delta = 3.8–3.6$ (m, 20H; $H_{b,c,d,e,f}$), 2.93 (t, 4H, $^3J = 6.7$ Hz, 4H; H_a), 1.71 (s, 2H; OH).

Methanesulfonic acid 2-{2-{2-[2-(2-methanesulfonyloxyethoxy)ethoxy]-ethyldisulanyl}ethoxy}ethoxy}ethyl ester (13): A solution of mesyl chloride (1.15 mL, 14.8 mmol) in CH_2Cl_2 (6 mL) was added dropwise under argon to a degassed solution of **12** (966 mg, 2.92 mmol) and triethylamine (4.52 mL, 32.4 mmol) at $-5\,^\circ$C in CH_2Cl_2. The temperature was maintained below $0\,^\circ$C during the addition. The mixture was stirred for 3 h at $-5\,^\circ$C before being brought to RT. The solution turned from colorless to pale yellow. It was washed with H_2O and dried over Na_2SO_4. After the solvent had been removed, a yellow oil was isolated and purified by flash column chromatography (SiO_2, eluent CH_2Cl_2/MeOH 0.5%). The product was obtained in 78% yield (929 mg, 2.01 mmol). **13**: Colorless oil. ^{1}H NMR (200 MHz, $CDCl_3$): $\delta = 4.38$ (m, 4H; H_f), 3.8–3.6 (m, 16H; $H_{b,c,d,e}$), 3.07 (s, 6H; CH_3), 2.88 (t, $^3J = 6.5$ Hz, 4H; H_a).

2-{2-[2-{2-[2-(2-Bromoethoxy)ethoxy]ethyldisulfanyl}ethoxy}ethoxy}bromoethane (9): A solution of **13** (384 mg, 0.831 mmol) in acetone (20 mL) was refluxed for 13 h in the presence of LiBr (820 mg, 9.46 mmol) under argon. After the solvent had been removed, the residue was taken up in CH_2Cl_2/H_2O. Extraction with CH_2Cl_2 and drying over Na_2SO_4 left, after evaporation of the solvent, a yellow oil (343 mg, 0.75 mmol) whose purity was good enough (> 95% by NMR) to be used without further purification. Yellow oil; ^{1}H NMR (200 MHz, $CDCl_3$): $\delta = 3.9–3.6$ (m, 16H; $H_{b,c,d,e}$), 3.48 (t, $^3J = 6$Hz, 4H; H_f), 2.89 (t, $^3J = 6.6$ Hz, 4H; H_a).

Threaded complex [Cu·(4)(6)]$^+$ and catenane [Cu·2]$^+$: By the cannula transfer technique, $[Cu(CH_3CN)_4]BF_4$ (207 mg, 0.66 mmol) in degassed acetonitrile (15 mL) was added under argon and at RT to a stirred, degassed pale yellow solution of macrocycle **4** (347 mg, 0.61 mmol) in CH_2Cl_2 (40 mL). A deep orange coloration appeared immediately. After 15 min at RT, a solution of 2,9-diphenol-1,10-phenanthroline (**6**; 221 mg, 0.61 mmol) in DMF (25 mL) was added by cannula to the solution, which instantly turned dark red. After the solution had been stirred for 30 min under argon at RT, the solvents were removed under high vacuum: precatenane [Cu(**4**)(**6**)]$^+$ was obtained as a dark red-brown powder. This product was dissolved in DMF (50 mL) with **9** (303 mg; 0.66 mmol). This degassed mixture was added dropwise over 24 h to a degassed solution of Cs_2CO_3 (601 mg, 1.84 mmol) in DMF (70 mL) at 58 °C. After addition, the solution was stirred for a further 12 h. The DMF was then removed, and the residue was taken up in CH_2Cl_2 and washed three times with water containing ascorbic acid, and three times with water. The organic layer was dried on Na_2SO_4, and the solvent was removed. Before purification, the counterions were exchanged from BF_4^- to PF_6^-. The product was then purified by several flash column chromatographies (Al_2O_3; eluent CH_2Cl_2) to give a dark red powder (118 mg; 15%). Small quantities of the less polar free macrocycle **8** were isolated too.

[Cu·2]PF$_6$: Dark red solid; ^{1}H NMR (400 MHz, ROESY, CD_2Cl_2): $\delta =$ 8.65 (d, $^3J = 8.4$ Hz, 2H; H_4), 8.56 (d, $^3J = 8.4$ Hz, 2H; $H_{4'}$), 8.24 (s, 2H; H_5), 8.18 (s, 2H; $H_{5'}$), 7.87 (d, $^3J = 8.4$ Hz, 2H; H_3), 7.85 (d, $^3J = 8.4$ Hz, 2H; $H_{3'}$), 7.39 (d, $^3J = 8.8$ Hz, 4H; H_o), 7.32 (d, $^3J = 8.8$ Hz, 4H; $H_{o'}$), 6.07 (d, $^3J =$ 8.8 Hz, 4H; H_m), 6.02 (d, $^3J = 8.8$ Hz, 4H; $H_{m'}$); 3.84 (m, 8H; H_ε, $H_{\varepsilon'}$), 3.72 (m, 20H; $H_{\alpha,\beta,\gamma,\delta,\delta'}$), 3.59 (m, 8H; $H_{\alpha',\gamma'}$); 3.48 (m, 4H; $H_{\beta'}$), 3.00 (t, $^3J =$ 6.4 Hz, 4H; H_ϕ); FAB-MS: found $m/z = 1287.3$ [$M^+ - PF_6$]; calcd: 1287.4.

Macrocycle 8: White solid; ^{1}H NMR (200 MHz, CD_2Cl_2): $\delta = 8.46$ (d, $^3J =$ 8.9 Hz, 4H; H_o), 8.24 (d, $^3J = 8.4$ Hz, 2H; H_4), 8.06 (d, $^3J = 8.4$ Hz, 2H; H_3), 7.73 (s, 2H; H_5), 7.15 (d, $^3J = 8.9$ Hz, 4H; H_m), 4.29 (t, $^3J = 5.0$ Hz, 4H; H_α), 3.94–3.66 (m, 16H; $H_{\beta,\gamma,\delta,\varepsilon}$), 2.97 (t, $^3J = 6.9$ Hz, 4H; H_ϕ); FAB-MS: found $m/z = 659.3$ [M^++H]; calcd: 658.8.

Threaded complex [Cu(6)(7)]$^+$ and catenane [Cu·3]$^+$: By the cannula transfer technique, $[Cu(CH_3CN)_4]BF_4$ (207 mg, 0.66 mmol) in degassed acetonitrile (15 mL) was added under argon and at RT to a stirred, degassed pale yellow solution of **7** (415 mg, 0.61 mmol) in CH_2Cl_2 (40 mL). A deep orange coloration appeared immediately. After 15 min at RT, a solution of 2,9-diphenol-1,10-phenanthroline (**6**, 222 mg, 0.61 mmol) in DMF (25 mL) was added by the cannula transfer technique to the solution, which immediately turned dark red. After the solution had been stirred for 30 min under argon at RT, the solvents were removed under high vacuum: precatenane [Cu(**6**)(**7**)]$^+$ was obtained as a dark red-brown powder. This product was dissolved in 50 mL DMF with **7** (303 mg, 0.66 mmol). This degassed mixture was added dropwise for 24 h to a degassed solution of Cs_2CO_3 (610 mg, 1.84 mmol) in DMF (70 mL) at 58 °C. After addition, the solution was stirred for a further 12 h. The DMF was then removed, and the residue was taken up in CH_2Cl_2 and washed three times with water containing ascorbic acid, and three times with water. The organic layer was dried over Na_2SO_4, and the solvent was removed. Before purification, the counter ions were exchanged from BF_4^- to PF_6^-.The product was then purified by several flash column chromatographies (SiO_2; CH_2Cl_2/2% MeOH) to give a dark red powder (112 mg, 12%). As in the case of the synthesis of [Cu·**2**]$^+$, small quantities of **8** were isolated.

[Cu·3]PF$_6$: Dark red solid; ^{1}H NMR (400 MHz, ROESY, CD_2Cl_2): $\delta =$ 8.70 (d, $^3J = 8.0$ Hz, 2H; H_{t3}), 8.62 (d, $^4J = 1.8$ Hz, 2H; H_{t6}), 8.49 (d, $^3J =$ 8.3 Hz, 2H; H_{t3}), 8.40 (d, $^3J = 8.4$ Hz, 2H; $H_{4'}$), 8.34 (d, $^3J = 8.3$ Hz, 2H; H_4), 8.08 (s, 4H; H_5, $H_{5'}$), 8.04 (t, $^3J = 8.0$ Hz,1H; H_{t4}), 7.80 (d, $^3J = 8.6$ Hz, 2H; $H_{3'}$), 7.68 (dd, $^3J = 8$ Hz, $^4J = 2$ Hz, 1H; H_{t4}), 7.66 (d, $^3J = 8.0$ Hz, 2H; H_3), 7.35 (d, $^3J = 8.5$ Hz, 4H; $H_{o'}$), 7.22 (d, $^3J = 8.5$ Hz, 4H; H_o), 5.99 (d, $^3J =$ 8.8 Hz, 4H; $H_{m'}$), 5.97 (d, $^3J = 8.8$ Hz, 4H; H_m), 3.84 (t, $^3J = 6.3$ Hz, 4H; H_α), 3.8–3.6 (m, 16H; $H_{\beta,\gamma,\delta,\varepsilon}$), 3.21 (t, $^3J = 7$ Hz, 4H; H_a), 2.99 (t, $^3J =$ 6.5 Hz, 4H; H_ϕ), 2.91 (m, 4H; H_b), 2.10 (m, 4H; H_c); MS (FAB-MS): found $m/z = 1398.3$ [$M^+ - PF_6$]; calcd: 1398.4.

[2]Catenane 3: [Cu·**3**]PF_6 (3.2 mg, 2.07 μmol) was dissolved in CH_2Cl_2 (3 mL). KCN (3 mg, 46 μmol) was dissolved in water (1 mL) and added to the former solution. The mixture was made homogeneous by addition of acetonitrile and stirred until the initial dark red color had totally disappeared (about 15 min). The mixture was then extracted with CH_2Cl_2, washed with water, and dried over Na_2SO_4. The water was discarded by pouring it into a solution of sodium hypochlorite. Evaporation of the solvent afforded the demetalated catenane **3**. Colorless solid; ^{1}H NMR (400 MHz, CD_2Cl_2): $\delta = 8.82$ (d, $^3J = 8$ Hz; 2H), 8.61 (d, $^4J = 2$ Hz; 2H), 8.45 (d, $^3J = 8$ Hz; 4H), 8.39 (d, $^3J = 8$ Hz; 2H), 8.3–7.9 (several signals; 13H), 7.77 (dd, $^3J = 8$ Hz, $^4J = 2$ Hz; 2H), 7.74 (s; 2H), 7.70 (s; 2H), 7.17 (d, $^3J = 9$ Hz; 4H), 7.06 (d, $^3J = 9$ Hz; 4H), 4.29 (br; 4H), 4.0 (t, $^3J = 6$ Hz; 4H), 4.0–3.5 (several signals; 16H), 2.95 (m; 4H), 2.79 (t, $^3J = 6$ Hz; 4H), 2.2 (m; 4H); MS (FAB-MS): found $m/z = 1337.4$ [M^++H], 678.2 [**7**$^+$ + H], 659.1 [**8**$^+$ + H]$^+$; calcd: 1337.6, 678.8, 659.8.

Cu(II) catenane [Cu·3]$^{2+}$: Catenane **3** (3 mg, 2.24 μmol) was dissolved in 5 mL CH_2Cl_2, the resulting solution completed to 10 mL by addition of acetonitrile. A slightly substoichiometric quantity of $Cu(BF_4)_2$ dissolved in acetonitrile was added. When the first drops of the copper(II) salt were added, the characteristic red color of the tetracoordinated Cu^I catenane appeared; further addition was rapidly accompanied by the appearance of the pale green color of the pentacoordinated Cu^{II} catenane. Evaporation of the solvents provided catenane [Cu·**3**]$(PF_6)_2$ as a pale green solid. Following the same procedure but using $Cu(ClO_4)_2$ instead of $Cu(BF4)_2$ yielded [Cu·**3**]$(ClO_4)_2$. Vis [Cu·**3**]$(ClO_4)_2$: $\lambda_{max} = 648$ nm, $\varepsilon =$ 180 mol^{-1} L cm^{-1} (CH_3CN).

Electrochemical experiments and adsorption procedure: Electrochemical experiments were carried out with an EGG Princeton 273A model potentiostat equipped with an $x-y$ recorder (Research Electrochemistry Software). All experiments were carried out at RT. For analytical experiments, a standard three-electrode cell was used. Potentials are referenced to an Ag wire pseudoreference electrode with 0.1 mol L^{-1} tetrabutylam-

monium tetrafluoroborate as supporting electrolyte in an acetonitrile/dichloromethane 4:1 mixture as solvent. To prevent any interaction with copper complexes and with the working gold electrode, use of electrolytes and reference electrodes containing chloride ions was avoided. The redox potentials of the adsorbed species were compared to those of the corresponding molecules in solution. With ferrocene as internal standard it was verified that the redox potential value of $[Cu(dpp)_2]^{2+/+}$ versus the Ag wire pseudoreference in acetonitrile is close to that versus the SCE reference electrode.[21] A platinum disc electrode (2 mm diameter) was used for CV experiments. The gold bead working electrodes were made by annealing the tip of a gold wire (99.9985%, 0.5 mm diameter) in a gas–oxygen flame. After being cooled, the hot gold bead was immersed in a 10^{-3} mol L^{-1} solution of the compound in CH_2Cl_2 for times varying from 10 min to 24 h. The electrode was then washed with pure CH_2Cl_2. Cyclic voltammetry (double compartment cell, Pt counter electrode, Ag wire pseudoreference electrode) was performed with the monolayer-covered working electrode immersed in 0.1 mol L^{-1} Bu_4NBF_4 (cell volume = 5 mL). The voltammetric response of these electrodes was checked when clean (before adsorption) in Bu_4NBF_4. Flat background responses in the potential range +0 V to 1 V versus Ag^+/Ag were commonly found.

General: Transition infrared spectra were recorded on a Perkin–Elmer 1725X FTIR spectrometer. PM-IRRAS was performed on a Nicolet Magna 860 FTIR spectrometer, equipped with a step-scan data collector, a photoelastic modulator, a lock-in amplifier and a MCT detector.[24, 25] The spectrometer was purged with dry nitrogen for 2 h before collection of the spectra. 1000 scans were recorded on each sample. STM imaging was performed at RT on a custom-made apparatus kindly donated by IBM Zurich Research Laboratory (Rüschlikon, Switzerland). Typical imaging conditions were 150–400 mV bias tip position and 10 pA current set point. Pt/Ir (80/20) cut tips were used. The AFM apparatus was a Nanoscope IIIa (Digital Instruments), equipped with a scanner capable of scanning a region of 16.8×16.8 μm. Experiments were carried out in air at RT. The images were recorded in tapping mode using a 225 μm long silicon cantilever (rectangular shape, $4\ \mathrm{mN\,m^{-1}} < k < 8\ \mathrm{mN\,m^{-1}}$, Nanoprobe GMBH).

Materials: Gold (99.99%) was obtained from Engelhard–Clal (Paris, France). Chromium (99.996%) was obtained from Johnson Matthey (Paris, France). Silicon wafers were purchased from ACM (Villiers, France). Chloroform used for SAM formation was distilled under nitrogen and degassed with nitrogen bubbling.

Substrates: Gold films (100 nm thick) were thermally evaporated and condensed onto glass slides that had been primed with chromium (2–4 nm) to promote gold adhesion. STM experiments were performed on flat Au(111) surfaces on mica prepared by deposition of 1000 Å of gold on a mica substrate heated to 350 °C. Such a process resulted in atomically flat terraces of up to 500×500 nm.

Monolayer formation: The SAM was formed by immersing gold substrates that had just been cleaned by UV–ozone treatment in a freshly prepared solution of the disulfide for 30 min. Then the substrate was rinsed with chloroform, dried, and immediately studied by PM-IRRAS.

Acknowledgements

We thank the French Ministry of Education for the fellowships to LR and CH, and the CNRS and the European Community for financial support.

[1] a) R. Ballardini, V. Balzani, M. T. Gandolfi, L. Prodi, M. Venturi, D. Philp, H. G. Ricketts, J. F. Stoddart, *Angew. Chem.* **1993**, *105*, 1362–1364; *Angew. Chem. Int. Ed. Engl.* **1993**, *32*, 1301–1303; b) V. Balzani, M. Gómez-López, J. F. Stoddart, *Acc. Chem. Res.* **1998**, *31*, 405–414; c) V. Balzani, A. Credi, F. M. Raymo, J. F. Stoddart, *Angew. Chem.* **2000**, *112*, 3486–3531; *Angew. Chem. Int. Ed.* **2000**, *39*, 3348–3391; d) C. P. Collier, G. Mattersteig, E. W. Wong, Y. Luo, K. Beverly, J. Sampaio, F. M. Raymo, J. F. Stoddart, J. R. Heath, *Science* **2000**, *289*, 1172–1175.

[2] J.-P. Sauvage, *Acc. Chem. Res.* **1998**, *31*, 611–619.

[3] a) J.-M. Kern, J.-P. Sauvage, G. Bidan, M. Billon, B. Divisia-Blohorn, *Adv. Mater.* **1996**, *8*, 580–582; b) G. Bidan, M. Billon, B. Divisia-Blohorn, J.-M. Kern, L. Raehm, J.-P. Sauvage, *New. J. Chem.* **1998**, 1134–1141; c) P.-L. Vidal, B. Divisia-Blohorn, G. Bidan, J.-L. Hazemann, J.-M. Kern, J.-P. Sauvage, *Chem. Eur. J.* **2000**, *6*, 1663–1673.

[4] a) T. Lu, L. Zhang, G. W. Gokel, A. E. Kaifer, *J. Am. Chem. Soc.* **1993**, *115*, 2542–2543; b) M. T. Rojas, A. E. Kaifer, *J. Am. Chem. Soc.* **1995**, *117*, 5883–5884.

[5] a) J.-M. Kern, L. Raehm, J.-P. Sauvage, *C.R. Acad. Sci. Ser. IIc* **1999**, 41–47; b) L. Raehm, C. Hamann, J.-M. Kern, J.-P. Sauvage, *Org. Lett.* **2000**, *14*, 1991–1994.

[6] a) A. Ulman, *Chem. Rev.* **1996**, *96*, 1533–1554, and references therein; b) A. N. Shipway, I. Willner, *Acc. Chem. Res.* **2001**, *34*, 421–432.

[7] a) M. Asakawa, M. Higuchi, G. Mattersteig, T. Nakamura, A. R. Pease, F. M. Raymo, T. Shimizu, J. F. Stoddart, *Adv. Mater.* **2000**, *12*, 1099–1102; b) S. Chia, J. Cao, J. F. Stoddart, J. I. Zink, *Angew. Chem.* **2001**, *113*, 2513–2517; *Angew. Chem. Int. Ed.* **2001**, *40*, 2447–2451.

[8] C. Dietrich-Buchecker, J.-P. Sauvage, J.-M. Kern, *J. Am. Chem. Soc.* **1984**, *106*, 3043–3045.

[9] J.-C. Chambron, in *Transition Metals in Supramolecular Chemistry* (Ed.: J.-P. Sauvage), Wiley, New York, **1999**, pp. 225–284.

[10] F. Arnaud-Neu, E. Marques, M.-J. Schwing-Weill, C. Dietrich-Buchecker, J.-P. Sauvage, J. Weiss, *New. J. Chem.* **1988**, *12*, 15–20.

[11] C. Dietrich-Buchecker, J.-P. Sauvage, *Tetrahedron* **1990**, *46*, 503–512.

[12] a) A. Livoreil, C. Dietrich-Buchecker, J.-P. Sauvage, *J. Am. Chem. Soc.* **1994**, *116*, 9399–9400; b) J.-P. Collin, P. Gavina, J.-P. Sauvage, *New. J. Chem.* **1997**, *21*, 525–528; c) J.-M. Kern, L. Raehm, J.-P. Sauvage, *Chem. Eur. J.* **1999**, *5*, 3310–3317.

[13] C. Dietrich-Buchecker, P. A. Marnot, J.-P. Sauvage, J.-P. Kintzinger, P. Maltèse, *Nouv. J. Chim.* **1984**, *8*, 573–582.

[14] W. Vetter, E. Logemann, G. Schill, *Org. Mass. Spectrom.* **1977**, *12*, 351–369.

[15] N. Armaroli, J.-C. Chambron, J.-P. Collin, C. Dietrich-Buchecker, L. Flamigni, J.-M. Kern, J.-P. Sauvage, in *Electron Transfer in Chemistry*, *Vol. 3* (Ed.: V. Balzani), Wiley-VCH, Weinheim, **2001**, pp. 582–654.

[16] This point is still controversial, but a large majority of the experimental evidence supports the actual cleavage of the S–S bond at the gold surface, leading subsequently to two Au–S bonds.

[17] J.-M. Kern, L. Raehm, J.-P. Sauvage, B. Divisia-Blohorn, P.-L. Vidal, *Inorg. Chem.* **2000**, *395*, 1555–1560.

[18] J. F. Rodriguez, T. Mebrahtu, M. P. Soriaga, *J. Electroanal. Chem.* **1987**, *233*, 283.

[19] Y. Saito, J. Takemoto, B. Hutchinson, K. Nakamoto, *Inorg. Chem.* **1972**, *11*, 2003.

[20] H. H. Perkampus, W. Rother, *Spectrochim. Acta* **1974**, *30A*, 597.

[21] C. O. Dietrich-Buchecker, J.-P. Sauvage, J.-M. Kern, *J. Am. Chem. Soc.* **1989**, *111*, 7791–7800.

[22] J. Kubas, *Inorganic Synthesis*, *Vol. 20*, Wiley, New York, **1979**, pp. 90–92.

[23] F. Guittard, E. Taffin de Givenchy, F. Szoenyi, A. Cambon, *Tetrahedron Lett.* **1995**, *36*, 7863–7866.

[24] T. Buffeteau, B. Desbat, J. M. Turlet, *Appl. Spectrosc.* **1991**, *45*, 380–389.

[25] A. Hatta, T. Wadayama, W. Suetaka, *Anal. Sci.* **1985**, *1*, 403–408.

Received: October 23, 2001 [F3636]

